Seismic Imaging of Sea-Floor Spreading

John C. Mutter

The globe-encircling filigree of mid-ocean ridges is the locus for the generation of new oceanic lithosphere by the process of sea-floor spreading. As part of this process molten magma rises to the surface from the deep mantle, freezes, and forms the basaltic oceanic crust. But molten magma could not have shot straight up from deep beneath the crust. Instead, it must have been stored for some period of time in a shallow level magma reservoir, or chamber, because the chemistry of volcanic rocks recovered from spreading centers is not consistent with magma having been in equilibrium with the parent mantle (*1*). Aspects of the lava chemistry also require shallow (low pressure) fractionation of magma (*2*). The heat required to drive the hydrothermal outflow on ridges seems to require shallow magma (*3*), and, perhaps most important, crustal magma chambers explain the structure of the only examples of oceanic crust that we can walk up to and inspect (*4*)—ophiolites. These are thought by many to be bona fide examples of crust produced at spreading centers and later impaled on land by tectonic forces. Studies of some ophiolites have also suggested that the magma body must be quite large, occupying perhaps two-thirds of the total crust (*5*).

These conclusions rely on strong but nevertheless inferential arguments: nobody can "see" a magma chamber in situ. The closest we come to viewing the internal structure of a spreading ridge is in the images produced by seismic methods. These can be created from reflected signals, just as we see ourselves reflected in a mirror with reflected light. Seismic energy travels as an elastic wave that is both reflected from and penetrates through the sea floor, enabling us to simultaneously "see" the sea floor and structure beneath—as if we could see the skin covering our face and the skeletal structure beneath at the same time. Energy transmitted through the crust can also be used to construct an image. In this approach the image is not directly available and must be constructed from particular properties of the wavefield. The closest analogy is the familiar medical application of computer axial tomography, better known as CAT scanning. For both reflected and transmitted images one can argue that the elastic properties of structures like magma bodies affect the seismic wavefield in detectable ways. The image is that of the distribution of quantities like the seismic wave propagation speed or the geometry of sharp impedance contrasts. The results from a number of recent seismic experiments, including those of Wilcock *et al.* on page 1470 of this issue, provide images of the structure of the sub-axial region of spreading centers, each with a different approach, and each providing a unique perspective on the process of sea-floor spreading (*6, 7, 9, 10, 12*).

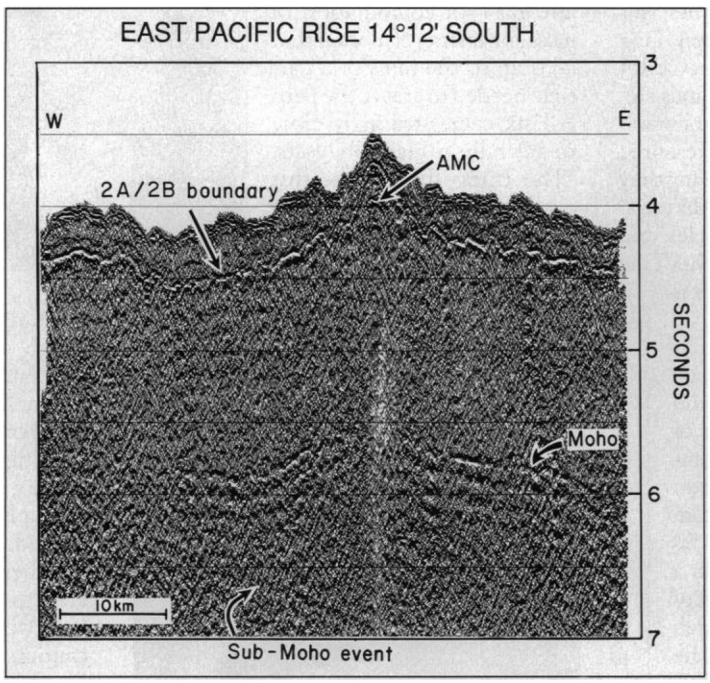

Fig. 1. The reflected response of the crust reveals sharp discontinuities such as the base of the extruded lavas (the 2A/2B boundary), the Moho at the base of the crust, and a small, bright reflection immediately beneath the crest of the Rise that marks a small pool of liquid magma, the Axial Magma Chamber (AMC).

Making use of these images to learn about the structure of spreading centers and particularly about the size, shape, and properties of a magma body requires another step. We have to translate the estimated physical quantity into a geological context. How does it help us understand the workings of a spreading system if we find, for instance, that the wave speed beneath a ridge is 5.3 km s^{-1}? One way to answer this is to briefly review what has been learned so far from several different types of seismic images (see Figs. 1 to 3).

The most easily accessible images are those created from the reflected response of the crust (Fig. 1). These look a lot like a simple cross section through the crust except that the vertical axis is not depth. It is a measure of the time taken by seismic energy to travel round-trip from the sea surface to the reflecting layer and back to the surface again. The spreading axis is an elevated region of the sea floor in the center of the image. The most distinct feature of the sub-surface is a shallow layer that approximately parallels the sea floor except immediately under the axis where it shallows considerably. Many investigators believe that this strong reflection probably marks the base of a layer of extruded lavas erupted at the ridge axis (*6, 7*) but the very distinct nature of the boundary is surprising and has yet to be fully explained. At deeper levels in the image we see the base of the crust marked by the Mohorovicic discontinuity, or Moho, and deeper still are indistinct features that may represent structure within the mantle.

The reflection image also shows a tiny bright signal from just below the rise axis (marked as AMC for Axial Magma Chamber in Figs. 1 and 2). The strength and spectral properties of the reflection suggest that it is the response of a body with much lower seismic wave speed than its surroundings and may therefore demark a liquid magma body (*8*). But there is no reflection from its base or its sides, so this image tells us little about its lateral extent. The reflection method images the response to relatively sharp changes in density or wave speed, or both. The reflection image implies either that the magma chamber is topped by a lens of liquid magma with sides and a base that are too gradational to appear, or that the tiny reflected signal represents the entire magma chamber. If the latter is the case, the size of the magma body is very much smaller than the indirect lines of evidence suggested.

What lies below the tiny, brightly reflected image becomes a key question. We can begin to get a sense of the nature of this zone from imaging techniques that make use of transmitted rather than reflected signals. These methods map long wavelength components of structure but analyze the ray paths and travel times of transmitted seismic waves—seismic CAT scans of the ridge. The

The author is at the Lamont-Doherty Geological Observatory, Palisades, NY 10964.

result is a cross-sectional image of the ridge's velocity field and can be constructed from results of a series of essentially one-dimensional experiments across the ridge (*9, 10*) or by seismic tomography which produces a true two-dimensional estimate of the seismic wave speed (*11, 12*).

Fig. 2. A two-dimensional image created by seismic tomography shows long wavelength features of the structure including a broad low-velocity region, much larger than the extent of the bright AMC reflection, that may contain a part liquid/part solid crystal mush. Image shows a region 6 by 16 km. [Adapted from (*12*)]

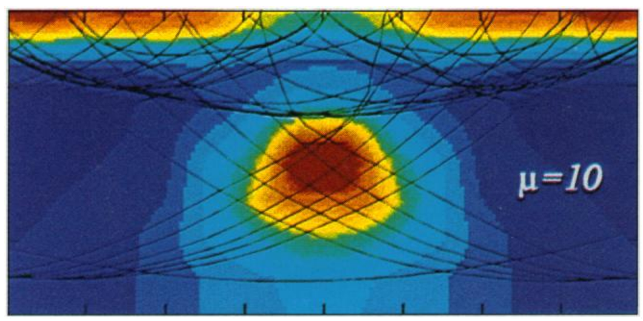

Fig. 3. The most recent image is that of the Q structure—the extent to which seismic energy is attenuated in its passage through the crust. Unlike other methods, the Q image is very sensitive to the presence of even small fractions of melt and holds promise for revealing the transitions between the liquid magma lens, the crystal mush, and the solid rock of the oceanic crust. Region shown is 8 km deep by 16 km wide.

These methods reveal a broad region of lowered velocities (Fig. 2) with an irregular shape that is often asymmetric. In the figure it lies somewhat to the left (west) of the rise axis. The image shown is a two-dimensional slice through a three-dimensional model of the axial region in which the shape of the low-velocity body and the degree of axial asymmetry change along the strike of the ridge, sometimes reflecting slight changes in the ridge's topography (*12*). Could this fluctuating image be providing evidence for the wide magma body suggested by ophiolite studies? The answer lies in how one interprets the velocity and what one means by the term "magma chamber."

If by magma chamber we mean a body of pure liquid, the answer is certainly "no." The seismic wave velocities in the larger body are low, but not low enough to represent a pure melt. Most would agree that pure melt, if present at all, occurs in a very thin lens immediately beneath the ridge axis, and that this lens lies at the summit of a region that contains a relatively small percentage of melt in a crystal matrix that may be capable of deformation, flow, and perhaps slow convection. Even though absolute melt percentage in this so-called crystal mush may be low, the melt could distribute throughout the mush in sufficient amounts and be sufficiently mobile that it could move easily to the surface to provide the source region for surface eruptions. As such it may be reasonable to regard the liquid lens and the mush zone as the magma chamber. The larger region of lowered velocities could correspond to a broad mush zone. Unfortunately seismic velocities are not very sensitive to the very small percentages of melt that are important to the overall properties of the mush (*13, 14*) and the tomographic images provide at best a fuzzy picture of the mush zone.

A potentially clearer, new type of seismic image is presented by Wilcock *et al.* (Fig. 3). Instead of measuring features of seismic propagation that respond to the elastic properties of crustal rocks, they estimate an anelastic property—the degree to which seismic energy is attenuated or absorbed in the crust. Anelastic attenuation is primarily the result of internal friction which causes dissipation of the energy into tiny amounts of heat. Rocks that have even a small density of cracks or pore spaces containing liquid depart considerably from perfect elasticity. Attenuative properties of crustal rocks near the solidus probably range through an order of magnitude, perhaps five times the range of the elastic property changes in the same region.

Attenuation is the energy loss per cycle (through anelastic processes) relative to peak energy at a given frequency (*15*) and must be estimated from the seismic waveforms themselves. Wilcock *et al.* use a spectral method to estimate the attenuation of waveforms. These data are then mapped into the distribution of crustal attenuation by means of a velocity model and ray paths derived from analysis of seismic travel times. Estimating attenuation therefore involves an extra step—all the information used in calculating the tomographic image is required together with the waveform data. Uncertainties involved in each step can compound and mitigate against the potential resolution of the attenuation image. Another caveat is that seismic waveforms change owing to elastic effects that can mimic the effects of anelastic attenuation (*16*). The image of Wilcock *et al.* is of apparent attenuation. From it they argue that the zone of crystal mush cannot occupy a region of more than a kilometer or so beneath the melt lens. Regions further from the lens may contain a very small percentage of melt or are formed of hot rock with no melt at all. Even using the generous definition of a magma chamber in which the mush zone is included, they find no support for a large magma body.

They also find that the shallow crustal layer becomes more attenuative as it thickens off-axis. Addition of volcanic material overflowing the axis and lapping down the flanks of the ridge seems to provide a likely explanation for the thickening and change in velocity structure (*7*) but the increase in attenuation cannot be satisfied by this mechanism alone. They argue that an in situ increase in porosity must also take place because of the effect of hydrothermal fluid movement in the upper crust.

Our knowledge of the processes that take place in the formation of oceanic crust is based on numerous types of observations, all of which must, in some sense, be inverted to provide estimates of the properties of crustal rocks. No single observational parameter provides the favored path to understanding these processes. Wilcock *et al.* have added another to the arsenal of research tools, one which holds great promise in sharpening our view of the substructure of spreading centers and elucidating the process of crustal genesis.

REFERENCES

1. W. B. Bryan *et al.*, *J. Geophys. Res.* **81**, 4285 (1976).
2. E. Stolper, *Contrib. Mineral. Petrol.* **74**, 7 (1980).
3. C. R. B. Lister, *Geophys. J. R. Astro. Soc.* **73**, 351 (1983).
4. J. F. Casey and J. A. Karson, *Nature* **198**, 295 (1981).
5. J. S. Palister and C. A. Hopson, *J. Geophys. Res.* **86**, 2593 (1981).
6. R. S. Detrick *et al.*, *Science*, in press.
7. A. J. Harding, G. M. Kent, J. A. Orcutt, *J. Geophys. Res.*, in press.
8. R. S. Detrick *et al.*, *Nature* **326**, 35 (1987).
9. E. E. Vera *et al.*, *J. Geophys. Res.* **95**, 15529 (1990).
10. A. J. Harding *et al.*, *ibid.* **94**, 12163 (1989).
11. D. W. Caress, M. S. Burnett, J. A. Orcutt, *ibid.* **97**, 9243 (1992).
12. D. R. Toomey, G. M. Purdy, S. C. Solomon, W. S. D. Wilcock, *Nature* **347**, 639 (1990).
13. T. Murase and A. R. McBirney, *Geol. Soc. Am. Bull.* **84**, 3563 (1973).
14. H. Sato, I. S. Sacks, T. Murase, *J. Geophys. Res.* **94**, 5689 (1989).
15. K. Aki and P. G. Richards, *Quantitative Seismology, Theory and Methods* (Freeman, San Francisco, 1980), p. 932.
16. P. G. Richards and W. Menke, *Bull. Seismol. Soc. Am.* **75**, 1005 (1983).